


Nuclear radii from total reaction cross section measurements at intermediate energies with complex turning point corrections to the eikonal model

Y. H. Wang,¹ D. Y. Pang^{1,*}, W. D. Chen¹, Y. P. Xu², W. L. Hai,¹ and R. Y. Chen¹

¹*School of Physics and Beijing Key Laboratory of Advanced Nuclear Materials and Physics, Beihang University, Beijing 100191, China*

²*School of Nuclear Science and Engineering, North China Electric Power University, Beijing 102206, China*

 (Received 9 August 2023; revised 17 December 2023; accepted 8 January 2024; published 24 January 2024)

Root mean square (rms) radii of light-heavy nuclei ${}^{6-9,11}\text{Li}$, ${}^{9-12}\text{Be}$, ${}^{10-15}\text{B}$, ${}^{11,12,14-18}\text{C}$, ${}^{14,16-19}\text{N}$, and ${}^{15,17,19-21}\text{O}$ are studied by analyzing the total reaction cross section data on a ${}^{\text{nat}}\text{Cu}$ target at intermediate energies within the range of 25–65 MeV/nucleon with the eikonal model. For calculations at such low and intermediate incident energies, the turning point corrections to the eikonal model, which effectively account for the distortions of the projectile trajectory caused by the Coulomb and/or nuclear forces, are examined with the elastic scattering angular distributions and total reaction cross sections of ${}^{16}\text{O}$ on ${}^{12}\text{C}$, ${}^{63}\text{Cu}$, and ${}^{208}\text{Pb}$ targets at incident energies from 12.5 to 200 MeV/nucleon. Effects of the corrections taking into account the turning points calculated with the Coulomb potential only, with both Coulomb and the real parts of the optical model potentials (OMPs), and with both the Coulomb and the complex OMPs, are evaluated by comparing with the exact results of partial wave Schrödinger equations. Complex turning point corrections are found to be important for light and intermediate-mass targets. With the complex turning point corrections, the rms radii obtained in this work differ, on average, from the results obtained from high-energy total interaction cross section measurements at around 650–1020 MeV/nucleon by 1.4%, which is much smaller than the averaged differences of 8% when no corrections to the eikonal model were made, and smaller than the averaged differences of 7.7% found in literature.

DOI: [10.1103/PhysRevC.109.014621](https://doi.org/10.1103/PhysRevC.109.014621)

I. INTRODUCTION

Root mean square radii of nucleon density distributions are basic bulk properties of atomic nuclei. Experiments with, for instance, the isotope shift method [1,2] and electron scattering [3–5] are able to provide precise information about nuclear charge radii. However, measurements with such electromagnetic probes are not always available for radioactive nuclei, which are very short-lived or are produced with very low intensity. Because of this, measurements of nuclear rms radii with hadronic probes, originating from the famous Rutherford experiment [6], are still valuable [7–9]. Unlike electromagnetic probes, which are only sensitive to the charge density distributions of atomic nuclei, hadronic probes also probe the neutron density distributions, which are important for nuclear structure and nuclear astrophysical studies [10–13].

Determining the rms radii of atomic nuclei using hadronic probes includes, for instance, elastic scattering angular distributions and/or total reaction cross sections induced by pions [14], protons [8,9], and α particles [7,10,15]. Since the mid 1980s, a lot of efforts have also been made with total reaction cross section and total interaction cross section measurements [16–18]. Essentially, all of these methods make use of folding models [19], which construct the projectile-target optical model potentials (OMPs) with effective pion-nucleon

or nucleon-nucleon interactions and nucleon density distributions (NDDs) of the projectile and/or the target nuclei. Assuming those effective interactions are known, the NDDs are varied so that the resulting OMPs can be used to reproduce the experimental data of elastic scattering angular distributions and/or total reaction/interaction cross sections, which, in turn, determines the rms radii of the nucleon density distributions of the projectile or the target nuclei. Root mean square radii obtained with these hadronic probes are inevitably model dependent [15,20]. In order to reduce the uncertainties in theoretical analysis, experiments were usually made at relatively high incident energies around several hundred MeV/nucleon and above. At these energies, the optical limit approximation of the Glauber model, which calculates the scattering phase shifts with parametrized free nucleon-nucleon total cross sections, ratios of the real and imaginary parts of the nucleon-nucleon scattering amplitudes, and finite-range parameters, has been found to be very simple yet successful in describing nuclear reactions induced by various nuclei [16,18,21].

However, there are also many experiments made at intermediate or low energies [22]. In Ref. [17], Saint-Laurent *et al.* reported their measurement of total reaction cross sections of many light heavy nuclei on a ${}^{\text{nat}}\text{Cu}$ target at incident energies within the range of 25–65 MeV/nucleon. RMS radii of these nuclei were studied by Liatard *et al.* with a Glauber-type analysis [23]. These rms radii are systematically larger than those obtained from the analysis of high-energy total

*dypang@buaa.edu.cn

interaction cross sections measured within the energy range of 650–1020 MeV/nucleon [18]. On average, the difference is about 7.7%. The reason for such a systematic difference is still unknown. It is important to know if it is possible to get consistent rms radii from total reaction/interaction measurements from high, intermediate, and low incident energies with the eikonal/Glauber model.

Over the years, low-energy corrections to the eikonal/Glauber model have been extensively studied from various aspects, for instance, the medium effects (density dependence) of the underlying nucleon-nucleon interaction/cross sections [24], the effects of Pauli blocking [25], and the effects of the momentum distributions of nucleon in nuclei [26]. These corrections are about the interactions used in eikonal/Glauber model calculations. One would expect that they could be effectively dealt with by (or simulated by) proper optical model potentials.

Another low-energy correction to the eikonal/Glauber model is about the straight-line trajectory assumption of the eikonal approximation. It is well known that such an assumption, which is valid at high energies, should be corrected due to the distortion of the projectile trajectories induced by the Coulomb and/or nuclear forces at low and intermediate incident energies. These are usually dealt with by the turning point correction (TPC) method [27–32]. These corrections are important for extending the range of applicability of the eikonal/Glauber model and for people to get consistent nuclear rms radii from nuclear reaction measurements within a wide range of incident energies. The literature of such corrections is quite long, but their effects on the deduced rms radii of the nucleon density distributions from total reaction cross sections measurements are, to our knowledge, not reported yet.

In this work, we study the rms radii of the ${}^{6-9,11}\text{Li}$, ${}^{9-12}\text{Be}$, ${}^{10-15}\text{B}$, ${}^{11,12,14-18}\text{C}$, ${}^{14,16-19}\text{N}$, and ${}^{15,17,19-21}\text{O}$ isotopes by re-analyzing the low and intermediate energy total reaction cross section measurements of Ref. [17] using the eikonal model with turning point corrections. The TPCs can be made by taking into account (1) the Coulomb potential only, (2) the Coulomb + real nuclear potentials, and (3) the Coulomb + complex nuclear potentials, e.g., the nuclear optical model potentials (OMPs). It will be shown that it is the last choice that allows one to get the best overall consistency between the rms radii obtained from these low and intermediate energy data and those from high-energy total interaction cross section data compiled in Ref. [18].

In the following text, we first briefly introduce the turning point corrections due to Coulomb and nuclear distortions in Sec. II. In order to determine which of the above-mentioned corrections best describes the experimental data, we systematically study the elastic scattering and total reaction cross sections of ${}^{16}\text{O}$ on ${}^{12}\text{C}$, ${}^{63}\text{Cu}$, and ${}^{208}\text{Pb}$, representing light, intermediate-mass, and heavy targets, respectively, at incident energies from 12.5 to 200 MeV/nucleon. The results are also shown in this section. We then study in Sec. III how the rms radii of the light-heavy isotopes change with and without making these corrections when they are required to produce the same total reaction cross section data. Our summary and conclusions are given in Sec. IV.

II. EIKONAL PHASE SHIFT AND TURNING POINT CORRECTIONS

A. The turning point

For a two-body projectile-target system, the eikonal model nuclear phase is [33]

$$\chi_N(\mathbf{b}) = -\frac{1}{\hbar v} \int_{-\infty}^{\infty} dz U_N(\mathbf{r}), \quad (1)$$

where \mathbf{b} is the impact parameter in the plane perpendicular to the z axis defined by the moving direction of the incident particle whose velocity is \mathbf{v} , $\mathbf{r} = \mathbf{b} + \mathbf{z}$ is the vector between the centers of mass of the projectile and the target nuclei, and $U_N(\mathbf{r})$ is the nuclear potential of this system. The Coulomb eikonal phase, χ_C , is [34]

$$\chi_C(b) = 2\eta \ln(kb), \quad (2)$$

where $k = \sqrt{2\mu E}/\hbar$ is the wave number in the center-of-mass system with μ and E being the reduced mass and the relative energies of the projectile-target system; $\eta = Z_1 Z_2 e^2/\hbar v$ is the Sommerfeld parameter with Z_1 and Z_2 being the charge numbers of the projectile and target nuclei. With χ_N and χ_C , the elastic scattering amplitudes can be calculated:

$$f_{el}(\theta) = f_C(\theta) + ik \int_0^{\infty} db b J_0(qb) e^{i\chi_C(b)} [1 - e^{i\chi_N(b)}], \quad (3)$$

where θ is the scattering angle in the center-of-mass system, $q = 2k \sin(\theta/2)$ is the momentum transfer, J_0 is the zeroth-order Bessel function, and $f_C(\theta)$ is the Coulomb scattering amplitude:

$$f_C(\theta) = -\frac{\eta}{2k \sin^2(\theta/2)} e^{-i\eta \ln[\sin^2(\theta/2)] + 2i\sigma_0(\eta)},$$

where $\sigma_0(\eta) = \arg \Gamma(1 + i\eta)$. With the eikonal model S -matrix defined as $S(b) = e^{i\chi_N(b)}$, the total reaction cross sections, σ_R , can be obtained by integration over the impact parameter b :

$$\sigma_R = 2\pi \int_0^{\infty} (1 - |S(b)|^2) b db. \quad (4)$$

The eikonal approximation assumes that a projectile goes through the field of a target nucleus along straight-line trajectories. This approximation is valid for high energy collisions. At lower incident energies, corrections have to be made to account for the distortion of the trajectories due to Coulomb and/or nuclear forces. This is usually done by replacing the impact parameters, b , with the distance of closest approach, d , which is a function of b , in the nuclear eikonal phase shift, $\chi_N(b) \rightarrow \chi_N(d)$, in calculating the elastic scattering and total reaction cross sections. The distance of closest approach d is called the turning point because at the distance $r = d$ the radial velocity of the projectile vanishes. For a given impact parameter b , which corresponds to an angular momentum $L = kb - 1/2$, the distance of closest approach d is the solution of the following equation [35]:

$$U(d) + \frac{L^2(b)}{2\mu d^2} - E = 0. \quad (5)$$

The turning point corrections to Glauber model calculations was proposed by Fäldt and Pilkuhn for pion-nucleus scattering [36]. It was applied to heavy-ion collisions by Vitturi and Zardi in Ref. [37] and later by many other groups [27–32].

B. Method of the turning point corrections

Three types of turning point corrections are usually made depending on what potentials are included in Eq. (5): (I) the Coulomb correction, with which only Coulomb potential is included, (II) Coulomb + real nuclear corrections, with which both Coulomb and nuclear potentials are included, but only the real part of the latter is taken into account, and (III) Coulomb + complex nuclear corrections with both real and imaginary parts of the nuclear potential taken into account. The type-I correction is rather commonly adopted in eikonal model calculations. Literature about the type-II correction is relatively limited [28–30]. Although it was discussed long ago in semiclassical scattering theory (see for instance Ref. [38]), application of the type-III correction in the analysis of heavy-ion scattering is still rather rare. To our knowledge, it has been reported only in three previous papers [27,31,32]. It is interesting to make a systematic study of the type-III correction and its effect on the extracted rms radii of light-heavy projectiles from total reaction cross section measurements. Following the notations in Ref. [31], the turning points corresponding to these three types of corrections are denoted as b_c , b' , and b'' , respectively. Clearly, the turning points b_c and b' are real, and b'' is complex.

Corrections with b_c and b' are usually made by substituting the impact factor b by b_c or b' in the nuclear eikonal phase: $\chi_N(b) \rightarrow \chi_N(b_c)$ or $\chi_N(b')$. When the turning points are complex, the corrections can still be made by substituting b with b'' in the eikonal phases, as was done by Aguiar, Zardi, and Vitturi [27], but they can also be made in another way. Considering $r = \sqrt{b^2 + z^2}$, the radius r becomes complex when the impact factor b is complex: $r'' = \sqrt{b''^2 + z^2}$. As discussed in Ref. [39], computing the nuclear potential with this complex distance r'' induces contributions from the real part of the OMP to the imaginary part of the eikonal shift χ_N (and the imaginary part of the OMP to the real part of χ_N as well) calculated with Eq. (1), which changes the ratio of the real and imaginary parts of χ_N , $\text{Re } \chi_N / \text{Im } \chi_N$. By choosing the imaginary part of r'' to have the same sign as the imaginary part of b'' , the ratio $\text{Re } \chi_N / \text{Im } \chi_N$ is enhanced, which enhances the absorption from the elastic scattering channel. We demonstrate the effect of the enhanced absorption with the case of ^{16}O elastic scattering from ^{12}C at an incident energy of 12.5 MeV/nucleon. As is shown in Fig. 1, the cross sections calculated without the turning point correction, represented by the dotted curve, deviate considerably from the exact result calculated with the partial wave Schrödinger equations, the solid curve. The eikonal model overestimates the exact result at large angles, which suggests that the uncorrected eikonal model lacks absorption from the elastic channel. Agreement with the exact result is greatly improved when the complex TPC is made, whose result is shown by the squares labeled as $U(r'')$, which corresponds to substituting r with r'' in Eq. (1) when calculating the nuclear eikonal

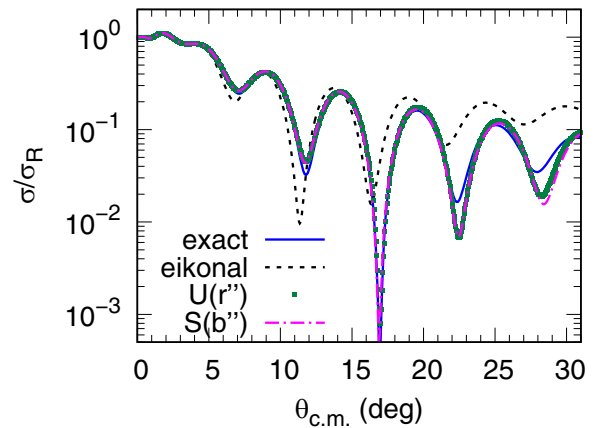


FIG. 1. Angular distributions of ^{16}O elastic scattering from ^{12}C at 12.5 MeV/nucleon. Curves are results of calculations with partial wave Schrödinger equations (the solid curve), with the eikonal model without corrections (the dotted curve), with the TPCs made on the optical potential $[U(r'')$, the squares], and with the TPCs made on the S matrix $[S(b'')$, the dash-dotted curve]. See text for the details.

phase. A standard Woods-Saxon type of OMP is used in these calculations, whose parameters are $V_r = -63.7$ MeV, $R_r = 5.1$ fm, $a_r = 0.63$ fm for the real part, and $W_i = -27.2$ MeV, $R_i = 5.1$ fm and $a_i = 0.69$ fm for the imaginary part. These parameters are from Ref. [27]. Clearly, one sees that the complex turning points corrections, which correspond to using complex radial distances r'' in the calculation of nuclear eikonal phase in Eq. (1), enhance absorption from the elastic scattering channel, thus improving the eikonal model for the description of the elastic scattering cross sections at low incident energies.

It is convenient to make the complex TPCs by substituting r with the corresponding complex r'' in Eq. (1) when the optical model potentials $U(r)$ are given in functional forms. However, for cases when functional forms of $U(r)$ are not given, for instance, when $U(r)$ are obtained with folding model calculations, it is more convenient to make the complex TPCs to the nuclear phase, $\chi_N(b)$, or to the S matrix, $S(b)$, directly, i.e., $\chi_N(b) \rightarrow \chi(b'')$ or $S(b) \rightarrow S(b'')$, as is done with b_c and b' corrections [28–30]. One question is, do results of the two approaches, namely, (1) by making $U(r) \rightarrow U(r'')$ substitution in Eq. (1), and (2) by making $\chi_N(b) \rightarrow \chi(b'')$ and $S(b) \rightarrow S(b'')$ in Eqs. (3) and (4), agree with each other? Our tests suggest that they do agree with each other satisfactorily. We demonstrate this again with the $^{16}\text{O} + ^{12}\text{C}$ case in Fig. 1. As shown by the dot-dashed curve, which was calculated by substituting b with b'' in $\chi_N(b)$ and $S(b)$, designated as $S(b'')$, agrees well with the results shown by the square symbols which were obtained by making the $U(r) \rightarrow U(r'')$ replacement, and they both improved the uncorrected eikonal model.

C. Effect of the TPCs to the elastic scattering and total reaction cross section calculations

In this section, we make a detailed examination of the effects of b_c , b' , and b'' corrections for heavy-ion collisions from low to high incident energies (up to 200 MeV/nucleon) and

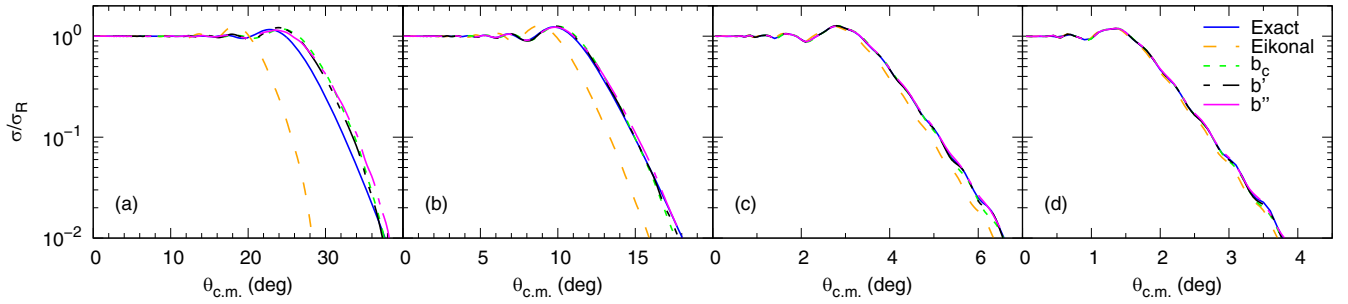


FIG. 2. Angular distributions as ratios to the Rutherford cross sections for ^{16}O elastic scattering from a ^{208}Pb target at incident energies of (a) 12.5 MeV/nucleon, (b) 25 MeV/nucleon, (c) 75 MeV/nucleon, and (d) 150 MeV/nucleon calculated with the partial wave Schrödinger equations, the eikonal model, and the eikonal model with turning point corrections. See the text for details.

from light to intermediate-mass and heavy targets. The cases studied are elastic scattering angular distributions and total reaction cross sections of a ^{16}O projectile on ^{12}C , ^{63}Cu , and ^{208}Pb , which represent light-heavy, intermediate, and heavy targets, respectively, at incident energies of 12.5, 25, 50, 75, 150, and 200 MeV/nucleon. For this, the systematic single folding model of the nucleus-nucleus potential (SFP) of Xu and Pang is used [40]. Although parameters of this potential were determined from elastic scattering data of ^6Li and ^7Li , the systematics of these parameters has been found to be applicable to many other heavier projectiles. This was demonstrated in Ref. [40] and by several more recent experiments with ^7Be , $^{8,10,13}\text{B}$, ^{9-11}C , ^{9-10}Be , and ^{13}O projectiles [41–46]. Here, the largest incident energy is set to be 200 MeV/nucleon because the systematic nucleon-nucleus potential parameters by Bauge *et al.* [47], from which the systematic SFPs are calculated, were given up to around 200 MeV/nucleon. Also, limiting the incident energies below 200 MeV/nucleon allows us to avoid the complication of relativistic corrections, which should be unnecessary in the present work because the main subject here is corrections to the eikonal model at low and intermediate energies.

Results with the ^{208}Pb target are shown in Fig. 2. Also shown are the exact results of partial wave Schrödinger equations. One sees that the Coulomb force is dominant in this case so the b_c correction plays the major role. Results of the b' and b'' corrections are very close to that of the b_c correction. These results agree well with those of Aguiar, Zardi, and Vitturi in Ref. [27]. One may conclude that all three corrections could produce results rather close to the exact ones for incident energies larger than around 25 MeV/nucleon on a target as

heavy as ^{208}Pb . One observes that all corrections overcorrected the exact results at the lowest examined incident energy, 12.5 MeV/nucleon, for a ^{208}Pb target. It will be interesting to see what caused such overcorrections and find a way to correct them back. But it is not the subject of the present work. We will be content when the corrections are sufficiently good for incident energies down to around 20 MeV/nucleon, which is about the lowest incident energies in the experiment of Ref. [17], whose results will be reanalyzed for the rms radii of light-heavy nuclei.

When the charge number of the target nucleus gets smaller, as the one shown in Fig. 3 for a ^{63}Cu target, Coulomb correction alone becomes insufficient to provide good agreement with the exact results. Nuclear corrections need to be taken into account. One important observation in this case is that both the real and imaginary parts of nuclear potentials have to be taken into account. This becomes more obvious on even lighter targets, for which the nuclear potentials become more important. As depicted in Fig. 4 for a ^{12}C target, taking only the real part of the nuclear potential (the b' correction) overestimated the exact results considerably at large angles. This suggests that additional absorption is needed to bring down the cross sections at large angles. As discussed in the previous section and in Ref. [39], it is effectively achieved by including the imaginary parts of the OMPs in Eq. (5). Satisfactory agreement with the exact results was found only when both the real and imaginary parts of the nuclear potentials were taken into account in the Coulomb + nuclear corrections.

The necessity of taking into account the full complex optical model potential in the TPC on light and

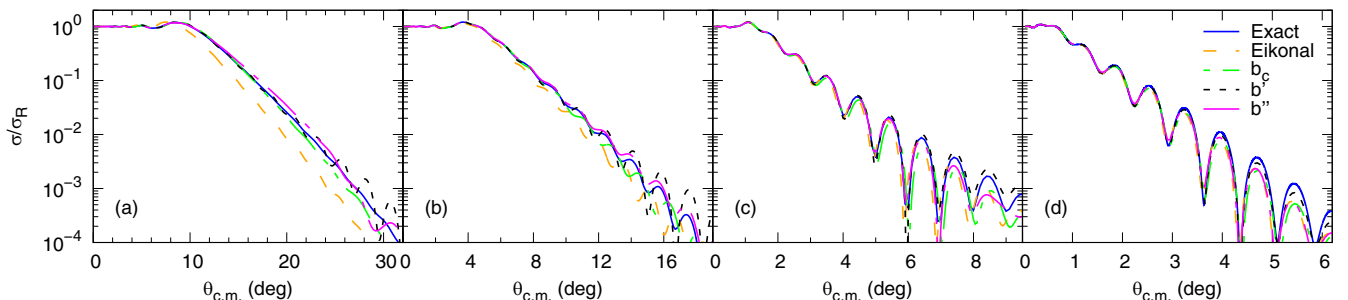
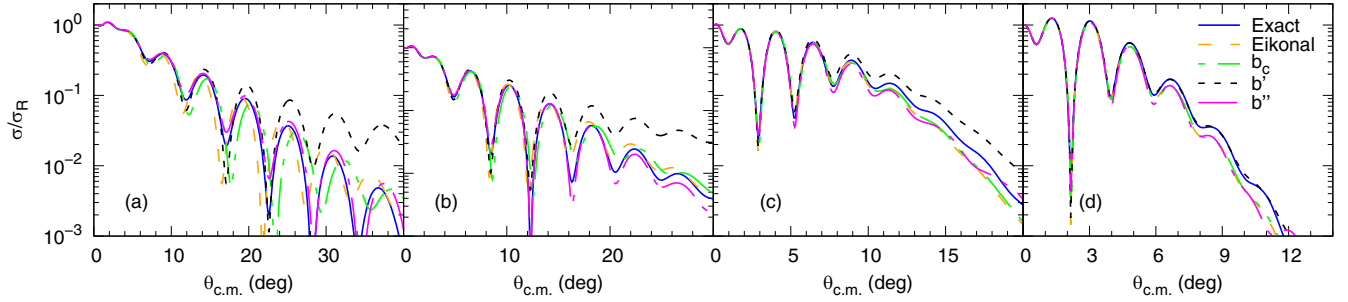


FIG. 3. The same as Fig. 2 but on a ^{63}Cu target.


 FIG. 4. The same as Fig. 2 but on a ^{12}C target.

intermediate-mass targets is more clearly seen in the total reaction cross sections (σ_R). This is demonstrated in Table. I, where σ_R calculated with the eikonal model, σ_{eik} , with the three types of turning point corrections, σ_{b_c} , $\sigma_{b'_c}$, and $\sigma_{b''}$, and with exact calculations, σ_{exact} , are listed. Comparisons of these cross sections are also depicted in Fig. 5, where the ratios $\sigma_{\text{eik}}/\sigma_{\text{exact}}$, $\sigma_{b_c}/\sigma_{\text{exact}}$, $\sigma_{b'_c}/\sigma_{\text{exact}}$, and $\sigma_{b''}/\sigma_{\text{exact}}$ are shown for the three targets at different incident energies. Again, one sees that the b'' correction provides the best agreement with the exact results.

III. RMS RADII FROM INTERMEDIATE ENERGY TOTAL REACTION CROSS SECTIONS

With the b'' correction proved successful to describe both the elastic scattering angular distributions and total

TABLE I. Total reaction cross sections of ^{16}O with ^{12}C , ^{63}Cu , and ^{208}Pb targets at incident energies $E_{\text{Lab}} = 12.5, 25, 50, 75, 150,$ and 200 MeV/nucleon calculated with partial wave Schrödinger equations, σ_{exact} , with the eikonal model, σ_{eik} , and with the three types of turning point corrections, σ_{b_c} , $\sigma_{b'_c}$, and $\sigma_{b''}$. See text for the details.

E_{lab}	σ_{exact}	σ_{eik}	σ_{b_c}	$\sigma_{b'_c}$	$\sigma_{b''}$
^{12}C					
12.5	1575.0	1701.6	1516.7	1555.0	1582.1
25	1512.2	1559.7	1471.4	1498.2	1522.7
50	1378.6	1391.8	1350.4	1369.0	1386.6
75	1264.6	1268.5	1242.3	1257.1	1271.0
150	1161.7	1162.8	1150.4	1157.5	1165.6
200	1152.5	1152.1	1142.8	1149.1	1155.5
^{63}Cu					
12.5	2457.7	3040.1	2395.4	2427.0	2453.3
25	2562.5	2829.2	2518.5	2542.3	2557.3
50	2487.0	2605.6	2456.8	2473.8	2486.7
75	2364.5	2435.8	2340.1	2354.1	2365.0
150	2261.1	2294.4	2248.1	2255.1	2262.6
200	2248.5	2271.2	2236.7	2243.6	2250.2
^{208}Pb					
12.5	3066.9	4977.2	2971.2	3008.6	3034.3
25	3782.0	4689.3	3716.0	3745.1	3780.0
50	3962.1	4387.5	3917.1	3938.8	3939.1
75	3883.1	4151.4	3846.7	3865.1	3862.9
150	3816.0	3944.6	3796.4	3805.8	3803.0
200	3818.6	3911.4	3800.7	3810.2	3808.0

reaction cross sections of light-heavy nuclei on the light and intermediate-mass targets, we reanalyze the intermediate-energy total reaction cross section data of Ref. [17] and study the rms radii of the $^{6-9,11}\text{Li}$, ^{9-12}Be , $^{10-15}\text{B}$, $^{11,12,14-18}\text{C}$, $^{14,16-19}\text{N}$, and $^{15,17,19-21}\text{O}$ isotopes with b'' corrections. The experiments were made with a ^{nat}Cu target, but we will assume it is a ^{63}Cu target in our calculations.

The optical model potentials are calculated again with the systematic SFP of Ref. [40]. These SFP calculations require the nucleon (proton and neutron) density distributions of the projectile and the nuclear matter density distribution of the target nuclei. So, to study the rms radii of the projectiles, we have to determine that of the target nucleus first. The nuclear matter density distribution of the ^{63}Cu target was determined by stretching the density distribution of

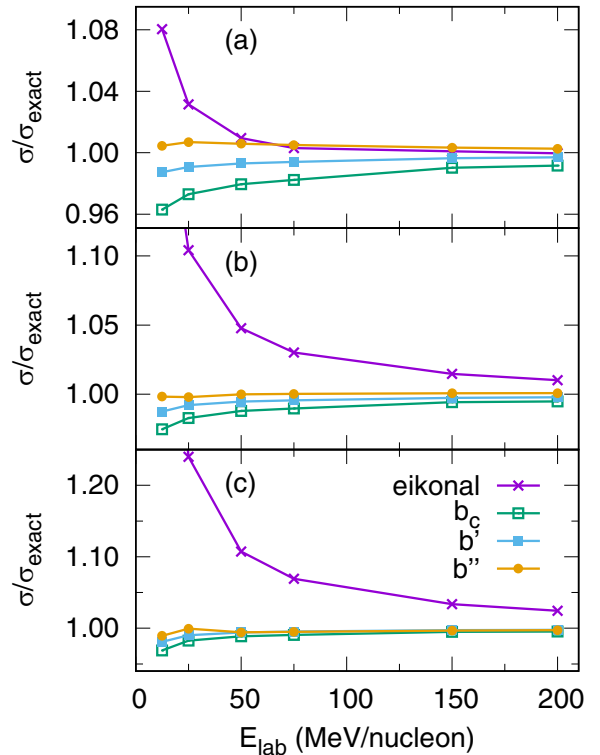


FIG. 5. Ratios of total reaction cross sections calculated with the eikonal model and the trajectory corrected eikonal model and the exact results for (a) ^{12}C , (b) ^{63}Cu , and (c) ^{208}Pb target at different incident energies. The lines are to guide eyes.

TABLE II. RMS radii of ${}^6\text{-}9,11\text{Li}$, ${}^9\text{-}12\text{Be}$, ${}^{10}\text{-}15\text{B}$, ${}^{11,12,14}\text{-}18\text{C}$, ${}^{14,16}\text{-}19\text{N}$, and ${}^{15,17,19}\text{-}21\text{O}$ isotopes from optical limit Glauber model (R_{OL}) analysis of interaction cross section measurements at high energies [18], from the Glauber model type analysis of total reaction cross sections measured at intermediate energies [17] by Liatard *et al.* [23] (R_{EL}), and from the analysis with the eikonal model and the b'' corrected eikonal model, R_{eik} and $R_{b''}$, respectively. X are the weighted means of $X_i = (R_i - R_{i,\text{OL}})/R_{i,\text{OL}}$ with weights $W_i = 1/[\Delta_{R_i}/R_i + \Delta_{R_{i,\text{OL}}}/R_{i,\text{OL}}]^2$ for each nucleus i , and Δ_X are the standard deviations of the corresponding X_i values. See text for the details.

A	R_{OL}	R_{EL}	R_{eik}	$R_{b''}$	A	R_{OL}	R_{EL}	R_{eik}	$R_{b''}$
Li					C				
6	2.32 ± 0.03	2.46 ± 0.21	1.96 ± 0.08	2.24 ± 0.09	14	2.30 ± 0.07	2.619 ± 0.057	2.11 ± 0.02	2.37 ± 0.02
7	2.33 ± 0.02	2.384 ± 0.023	2.07 ± 0.02	2.22 ± 0.02	15	2.40 ± 0.05	2.783 ± 0.092	2.35 ± 0.04	2.59 ± 0.04
8	2.37 ± 0.02	2.583 ± 0.023	2.33 ± 0.01	2.48 ± 0.01	16	2.70 ± 0.03	2.756 ± 0.058	2.29 ± 0.02	2.56 ± 0.02
9	2.32 ± 0.02	2.534 ± 0.025	2.12 ± 0.01	2.26 ± 0.01	17	2.72 ± 0.03	3.04 ± 0.11	2.79 ± 0.06	3.00 ± 0.06
11	3.12 ± 0.16	2.779 ± 0.071	2.59 ± 0.03	2.74 ± 0.03	18	2.82 ± 0.04	2.9 ± 0.19	2.52 ± 0.09	2.76 ± 0.10
Be					N				
9	2.38 ± 0.01	2.53 ± 0.072	2.09 ± 0.03	2.30 ± 0.03	14	2.47 ± 0.03	2.61 ± 0.10	1.88 ± 0.05	2.34 ± 0.06
10	2.30 ± 0.02	2.479 ± 0.028	2.15 ± 0.01	2.37 ± 0.01	16	2.50 ± 0.10	2.71 ± 0.28	2.24 ± 0.02	2.50 ± 0.02
11	2.73 ± 0.05	3.039 ± 0.038	2.83 ± 0.24	2.94 ± 0.25	17	2.48 ± 0.05	2.795 ± 0.039	2.42 ± 0.02	2.70 ± 0.03
12	2.59 ± 0.06	2.622 ± 0.073	2.35 ± 0.03	2.63 ± 0.03	18	2.65 ± 0.02	2.803 ± 0.041	2.42 ± 0.02	2.72 ± 0.03
B					19	2.71 ± 0.03	2.786 ± 0.054	2.34 ± 0.03	2.63 ± 0.03
10	2.20 ± 0.06	2.56 ± 0.23	2.05 ± 0.10	2.44 ± 0.12	O				
11	2.09 ± 0.12	2.605 ± 0.09	2.28 ± 0.04	2.49 ± 0.04	15	2.44 ± 0.04	2.70 ± 0.38	2.09 ± 0.26	2.51 ± 0.31
12	2.39 ± 0.02	2.723 ± 0.048	2.31 ± 0.02	2.55 ± 0.02	17	2.59 ± 0.05		1.91 ± 0.04	2.50 ± 0.05
13	2.46 ± 0.12	2.746 ± 0.048	2.26 ± 0.02	2.50 ± 0.02	19	2.68 ± 0.03	2.58 ± 0.30	2.30 ± 0.31	2.95 ± 0.39
14	2.44 ± 0.06	3.00 ± 0.10	2.70 ± 0.05	2.89 ± 0.06	20	2.69 ± 0.03	3.00 ± 0.35	2.61 ± 0.02	2.91 ± 0.02
15	2.45 ± 0.27	2.61 ± 0.19	2.46 ± 0.27	2.74 ± 0.30	21	2.71 ± 0.03	2.76 ± 0.19	2.19 ± 0.08	2.54 ± 0.09
C									
11	2.12 ± 0.06	2.46 ± 0.3	1.73 ± 0.17	2.13 ± 0.21	X (%)		7.7	-8.0	1.4
12	2.31 ± 0.02	2.481 ± 0.08	1.81 ± 0.04	2.25 ± 0.05	Δ_X (%)		7.1	8.8	7.3

${}^{63}\text{Cu}$, $\rho(r) \rightarrow \rho(r/a)/a^3$, which increases/decreases its rms radius by a factor of a while keeping its normalization unchanged, so that σ_R of the $\alpha + {}^{63}\text{Cu}$ system calculated with the single-folding model α -particle potential of Ref. [48] using the stretched target density is consistent with the experimental one reported in Ref. [17]. Hartree-Fock (HF) calculation using the SkX interaction [49] is done for the original $\rho(r)$. The proton, neutron, and charge density distributions of the HF calculations are stretched simultaneously. The so obtained rms charge radius of ${}^{63}\text{Cu}$ is 3.968 fm, which is very close to the experimental one of 3.932 ± 0.022 fm of ${}^{\text{nat}}\text{Cu}$ measured with electron scattering [50]. This corresponds to a 3.896 fm rms radius of the nuclear matter distribution of ${}^{63}\text{Cu}$.

With the nucleon density distributions of the ${}^{63}\text{Cu}$ target fixed, we determine the rms radii of the ${}^6\text{-}9,11\text{Li}$, ${}^9\text{-}12\text{Be}$, ${}^{10}\text{-}15\text{B}$, ${}^{11,12,14}\text{-}18\text{C}$, ${}^{14,16}\text{-}19\text{N}$, and ${}^{15,17,19}\text{-}21\text{O}$ isotopes with the following procedure: (1) calculate the SFP with NDD of the projectile from HF calculations using the SkX interaction, $\rho_{p,n}^{\text{HF}}(r)$, (2) calculate the σ_R value with the b'' correction of the eikonal model using this SFP, (3) repeat stretching or squeezing $\rho_{p,n}^{\text{HF}}(r)$ and calculate the SFP and σ_R until the calculated σ_R agrees with its experimental counterpart. The rms radius of the projectile, R_p , is then determined from the stretched/squeezed NDD. The uncertainty of the so determined rms radius, Δ_{R_p} , is calculated using the uncertainty of the experimental data Δ_{σ_R} reported in Ref. [17]: $\Delta_{R_p} = R_p \times \Delta_{\sigma_R}/2\sigma_R$. For projectiles which have σ_R values measured at more than one incident

energy, the rms radii are taken to be the weighted averages of the R_p values with $1/\Delta_{R_p}^2$ being the weights. The final results are listed in Table II. For comparison purpose, the rms radii determined using the uncorrected eikonal model and those obtained by E. Liatard *et al.* using a Glauber-model-like analysis in Ref. [23] are also shown.

Each experimental datum has its own uncertainties. So it should be more meaningful to compare the *averaged* differences among results of different measurements/analysis than to compare the results of any specific nucleus in systematic studies. The last two lines of Table II are the weighted averages (X) and the standard deviations of the differences (Δ_X) between the rms radii obtained from the intermediate energy data and their corresponding values from optical limit Glauber model analysis of total interaction cross sections measured at higher energies within the range of 650–1020 MeV/nucleon [18]. One sees that, on average, the uncorrected eikonal model underestimated the high energy results by $X = -8.0\%$. With the b'' correction, X is greatly reduced to 1.4%. On the other hand, the X value of the results in Ref. [23] is 7.7%. The standard deviations of these differences in the three cases are, however, rather close. The above comparisons are more clearly seen in Figs. 6 and 7. For the sake of clarity, results of the uncorrected eikonal model listed in Table II are not plotted. Note that possible detection problems were discussed in Ref. [23] for the measured σ_R value of ${}^{11}\text{Li}$ due to its weakly bound nature. Similar problems may exist for other weakly

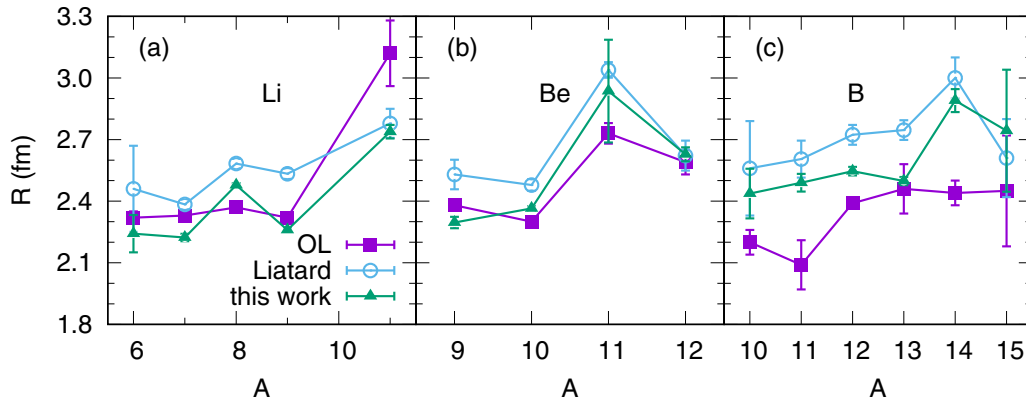


FIG. 6. RMS radii of (a) ${}^{6-9,11}\text{Li}$, (b) ${}^{9-12}\text{Be}$, and (c) ${}^{10-15}\text{B}$ isotopes from interaction cross sections measured at high energies analyzed with the optical limit Glauber model (OL) [18] and from total reaction cross sections measured at intermediate energies [17] obtained by Liatard *et al.* (Liatard) [23] and in this work. See the text for details.

bound nuclei, such as ${}^{11}\text{Be}$, ${}^{14}\text{B}$, and ${}^{17}\text{C}$, whose neutron separation energies are smaller than 1.0 MeV. The X values become -8.5% , 1.1% , and 7.4% , respectively, when these four weakly bound nuclei are excluded in the analysis, which makes the b'' correction even more appealing. The systematic difference between results of Ref. [23] from intermediate-energy total reaction cross section data and those compiled in Ref. [18] from high-energy total interaction data has been left unexplained for more than three decades. Since the theoretical analyses made in Ref. [23] are rather different from what we make here, both in the adopted nuclear interactions and in the manipulation of nucleon density distributions, we do not endeavor to pin down the origin(s) of the differences between our results and those of Ref. [23]. The important information we get here is that, with the b'' correction, one is able to get, globally, rather consistent rms radii of light-heavy nuclei from low- and intermediate-energy nuclear reaction data and from high-energy total reaction/interaction cross section data.

IV. SUMMARY

Low energy corrections to the eikonal approximation is important for systematic studies of nuclear reactions with the eikonal/Glauber model within a wide range of incident energies. In this work, we study the turning point corrections

to the eikonal model and its effect on the rms radii of some light-heavy projectile from low- and intermediate-energy total reaction cross sections measurements. We firstly systematically examined the effects of TPCs due to the Coulomb force only and to both Coulomb and nuclear potentials (with real their parts only or with both real and imaginary parts) with the elastic scattering angular distributions and total reaction cross sections of the ${}^{16}\text{O}$ projectile on ${}^{12}\text{C}$, ${}^{63}\text{Cu}$, and ${}^{208}\text{Pb}$ targets at incident energies from 12.5 to 200 MeV/nucleon. We demonstrate that the TPC taking into account both the real and imaginary parts of the optical model potential, namely, the complex TPC, provides the best agreement with the exact results. This is especially important on light and intermediate-mass targets.

By applying the complex TPCs to the eikonal approximation, total reaction cross sections of ${}^{6-9,11}\text{Li}$, ${}^{9-12}\text{Be}$, ${}^{10-15}\text{B}$, ${}^{11,12,14-18}\text{C}$, ${}^{14,16-19}\text{N}$, and ${}^{15,17,19-21}\text{O}$ isotopes on a ${}^{\text{nat}}\text{Cu}$ target at intermediate incident energies measured by Saint-Laurent *et al.* [17] were reanalyzed and the rms radii of nucleon density distributions of these light-heavy projectiles were obtained. The averaged differences between our results and those obtained from high-energy total interaction cross section measurements compiled by Ozawa *et al.* in Ref. [18] is 1.4% , which is much smaller than the averaged difference of -8.0% from the uncorrected eikonal model calculation

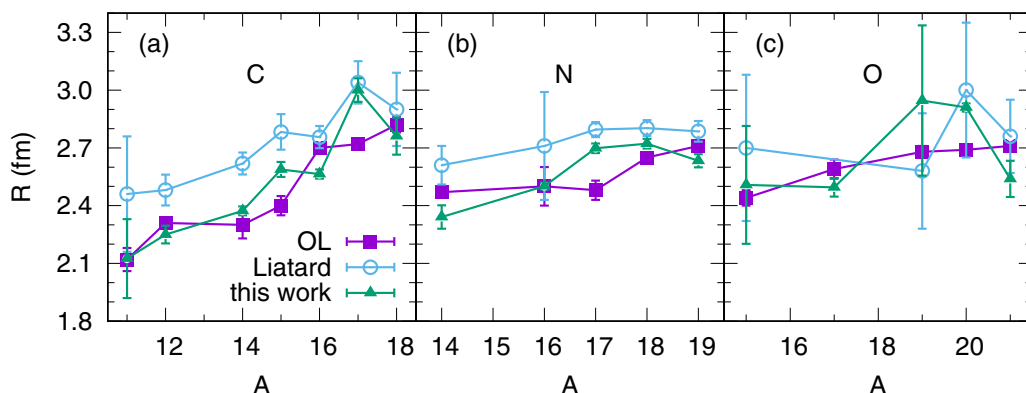


FIG. 7. The same as Fig. 6 but for (a) ${}^{11,12,14-18}\text{C}$, (b) ${}^{14,16-19}\text{N}$, and (c) ${}^{15,17,19-21}\text{O}$ isotopes.

and of 7.7% from the results of Liatard *et al.* in Ref. [23]. This suggests that rms radii of light-heavy nuclei obtained from total reaction cross section measurements at low and intermediate incident energies can be rather consistent with those obtained from high-energy total interaction/reaction cross section measurements when complex TPCs are made in the eikonal/Glauber model calculations. One could expect that the complex TPC would also be important for analysis

of other types of reactions, such as single nucleon removal reactions [51], with the eikonal/Glauber model at low and intermediate energies on light targets.

ACKNOWLEDGMENT

This work is supported by the National Natural Science Foundation of China (Grant No. U2067205).

-
- [1] A. Koszorús, X. F. Yang, W. G. Jiang, S. J. Novario, S. W. Bai, J. Billowes, C. L. Binnersley, M. L. Bissell, T. E. Cocolios, B. S. Cooper, R. P. de Groote, A. Ekström, K. T. Flanagan, C. Forssén, S. Franchoo, R. F. G. Ruiz, F. P. Gustafsson, G. Hagen, G. R. Jansen, A. Kanellakopoulos *et al.*, *Nat. Phys.* **17**, 439 (2021).
- [2] X. Yang, S. Wang, S. Wilkins, and R. G. Ruiz, *Prog. Part. Nucl. Phys.* **129**, 104005 (2023).
- [3] G. Fricke, C. Bernhardt, K. Heilig, L. Schaller, L. Schellenberg, E. Spera, and C. Dejager, *At. Data Nucl. Data Tables* **60**, 177 (1995).
- [4] K. Tsukada, A. Enokizono, T. Ohnishi, K. Adachi, T. Fujita, M. Hara, M. Hori, T. Hori, S. Ichikawa, K. Kurita, K. Matsuda, T. Suda, T. Tamae, M. Togasaki, M. Wakasugi, M. Watanabe, and K. Yamada, *Phys. Rev. Lett.* **118**, 262501 (2017).
- [5] T. Suda, *J. Phys.: Conf. Ser.* **2391**, 012004 (2022).
- [6] E. Rutherford, *Philosophical Mag. J. Sci.* **21**, 669 (1911).
- [7] H. J. Gils, H. Rebel, and E. Friedman, *Phys. Rev. C* **29**, 1295 (1984).
- [8] S. Terashima, H. Sakaguchi, H. Takeda, T. Ishikawa, M. Itoh, T. Kawabata, T. Murakami, M. Uchida, Y. Yasuda, M. Yosoi, J. Zenihiro, H. P. Yoshida, T. Noro, T. Ishida, S. Asaji, and T. Yonemura, *Phys. Rev. C* **77**, 024317 (2008).
- [9] J. Zenihiro, H. Sakaguchi, T. Murakami, M. Yosoi, Y. Yasuda, S. Terashima, Y. Iwao, H. Takeda, M. Itoh, H. P. Yoshida, and M. Uchida, *Phys. Rev. C* **82**, 044611 (2010).
- [10] H. J. Gils and H. Rebel, *Phys. Rev. C* **13**, 2159 (1976).
- [11] X. Roca-Maza, M. Centelles, X. Viñas, and M. Warda, *Phys. Rev. Lett.* **106**, 252501 (2011).
- [12] M. B. Tsang, J. R. Stone, F. Camera, P. Danielewicz, S. Gandolfi, K. Hebeler, C. J. Horowitz, J. Lee, W. G. Lynch, Z. Kohley, R. Lemmon, P. Möller, T. Murakami, S. Riordan, X. Roca-Maza, F. Sammarruca, A. W. Steiner, I. Vidaña, and S. J. Yennello, *Phys. Rev. C* **86**, 015803 (2012).
- [13] W. Horiuchi, Y. Suzuki, and T. Inakura, Probing neutron-skin thickness of unstable nuclei with total reaction cross sections, in *Proceedings of the Conference on Advances in Radioactive Isotope Science (ARIS2014)* [JPS Conf. Proc. 6, 030080 (2015)].
- [14] M. J. Jakobson, G. R. Bureson, J. R. Calarco, M. D. Cooper, D. C. Hagerman, I. Halpern, R. H. Jeppeson, K. F. Johnson, L. D. Knutson, R. E. Marrs, H. O. Meyer, and R. P. Redwine, *Phys. Rev. Lett.* **38**, 1201 (1977).
- [15] J. Gils, E. Friedman, and H. Rebel, *Radial Sensitivity of Hadronic Probes and how Accurately are Nuclear radii Determined*, Technical Report No. KfK 3039 (Institut für Angewandte Kernphysik, Karlsruhe, 1980).
- [16] I. Tanihata, H. Hamagaki, O. Hashimoto, Y. Shida, N. Yoshikawa, K. Sugimoto, O. Yamakawa, T. Kobayashi, and N. Takahashi, *Phys. Rev. Lett.* **55**, 2676 (1985).
- [17] M. Saint-Laurent, *Z. Phys. A, At. Nucl.* **332**, 457 (1989).
- [18] A. Ozawa, T. Suzuki, and I. Tanihata, *Nucl. Phys. A* **693**, 32 (2001), special issue, Radioactive Nuclear Beams.
- [19] G. Satchler and W. Love, *Phys. Rep.* **55**, 183 (1979).
- [20] M. M. Sternheim and K.-B. Yoo, *Phys. Rev. Lett.* **41**, 1781 (1978).
- [21] W. Horiuchi, Y. Suzuki, B. Abu-Ibrahim, and A. Kohama, *Phys. Rev. C* **75**, 044607 (2007).
- [22] D. T. Tran, H. J. Ong, T. T. Nguyen, I. Tanihata, N. Aoi, Y. Ayyad, P. Y. Chan, M. Fukuda, T. Hashimoto, T. H. Hoang, E. Ideguchi, A. Inoue, T. Kawabata, L. H. Khiem, W. P. Lin, K. Matsuta, M. Mihara, S. Momota, D. Nagae, N. D. Nguyen (RCNP-E372 Collaboration) *et al.*, *Phys. Rev. C* **94**, 064604 (2016).
- [23] E. Liatard, J. F. Bruandet, F. Glasser, S. Kox, T. U. Chan, G. J. Costa, C. Heitz, Y. E. Masri, F. Hanappe, R. Bimbot, D. Guillemaud-Mueller, and A. C. Mueller, *Europhys. Lett.* **13**, 401 (1990).
- [24] X. Cai, J. Feng, W. Shen, Y. Ma, J. Wang, and W. Ye, *Phys. Rev. C* **58**, 572 (1998).
- [25] M. Hussein, R. Rego, and C. Bertulani, *Phys. Rep.* **201**, 279 (1991).
- [26] M. Takechi, M. Fukuda, M. Mihara, K. Tanaka, T. Chinda, T. Matsumasa, M. Nishimoto, R. Matsumiya, Y. Nakashima, H. Matsubara, K. Matsuta, T. Minamisono, T. Ohtsubo, T. Izumikawa, S. Momota, T. Suzuki, T. Yamaguchi, R. Koyama, W. Shinozaki, M. Takahashi *et al.*, *Phys. Rev. C* **79**, 061601(R) (2009).
- [27] C. E. Aguiar, F. Zardi, and A. Vitturi, *Phys. Rev. C* **56**, 1511 (1997).
- [28] S. K. Gupta and P. Shukla, *Phys. Rev. C* **52**, 3212 (1995).
- [29] P. Shukla, *Phys. Rev. C* **67**, 054607 (2003).
- [30] A. Mehndiratta and P. Shukla, *Nucl. Phys. A* **961**, 22 (2017).
- [31] C. Hebborn and P. Capel, *Phys. Rev. C* **96**, 054607 (2017).
- [32] C. Hebborn and P. Capel, *Phys. Rev. C* **98**, 044610 (2018).
- [33] C. Bertulani and P. Danielewicz, *Introduction to Nuclear Reactions* (CRC, Boca Raton, 2004).
- [34] C. Bertulani, C. Campbell, and T. Glasmacher, *Comput. Phys. Commun.* **152**, 317 (2003).
- [35] P. Fröbrich and R. Lipperheide, *Theory of Nuclear Reactions*, Oxford Science Publications (Clarendon, Oxford, 1996).
- [36] G. Fäldt and H. Pilkuhn, *Phys. Lett. B* **46**, 337 (1973).
- [37] A. Vitturi and F. Zardi, *Phys. Rev. C* **36**, 1404 (1987).
- [38] D. Brink, *Semi-Classical Methods in Nucleus-Nucleus Scattering* (Cambridge University Press, Cambridge, 1985).
- [39] C. Hebborn, Study of the eikonal approximation to model exotic reactions, Ph.D. thesis, Université Libre de Bruxelles, 2020 (unpublished).
- [40] Y. P. Xu and D. Y. Pang, *Phys. Rev. C* **87**, 044605 (2013).

- [41] Y. Y. Yang, J. S. Wang, Q. Wang, D. Pang, J. B. Ma, M. R. Huang, J. L. Han, P. Ma, S. L. Jin, Z. Bai, Q. Hu, L. Jin, J. B. Chen, N. Keeley, K. Rusek, R. Wada, S. Mukherjee, Z. Y. Sun, R. F. Chen, X. Y. Zhang *et al.*, *Phys. Rev. C* **87**, 044613 (2013).
- [42] Y. Y. Yang, J. S. Wang, Q. Wang, D. Y. Pang, J. B. Ma, M. R. Huang, P. Ma, S. L. Jin, J. L. Han, Z. Bai, L. Jin, J. B. Chen, Q. Hu, R. Wada, S. Mukherjee, Z. Y. Sun, R. F. Chen, X. Y. Zhang, Z. G. Hu, X. H. Yuan *et al.*, *Phys. Rev. C* **90**, 014606 (2014).
- [43] Y. Y. Yang, X. Liu, D. Y. Pang, D. Patel, R. F. Chen, J. S. Wang, P. Ma, J. B. Ma, S. L. Jin, Z. Bai, V. Guimarães, Q. Wang, W. H. Ma, F. F. Duan, Z. H. Gao, Y. C. Yu, Z. Y. Sun, Z. G. Hu, S. W. Xu, S. T. Wang *et al.*, *Phys. Rev. C* **98**, 044608 (2018).
- [44] Y. Shen, B. Guo, T. Ma, D. Pang, D. Ni, Z. Ren, Y. Li, Z. An, J. Su, J. Liu, Q. Fan, Z. Han, X. Li, Z. Li, G. Lian, Y. Su, Y. Wang, S. Yan, S. Zeng, and W. Liu, *Phys. Lett. B* **797**, 134820 (2019).
- [45] F. Duan, Y. Yang, K. Wang, A. Moro, V. Guimarães, D. Pang, J. Wang, Z. Sun, J. Lei, A. Di Pietro, X. Liu, G. Yang, J. Ma, P. Ma, S. Xu, Z. Bai, X. Sun, Q. Hu, J. Lou, X. Xu *et al.*, *Phys. Lett. B* **811**, 135942 (2020).
- [46] K. Wang, Y. Y. Yang, V. Guimarães, D. Y. Pang, F. F. Duan, Z. Y. Sun, J. Lei, G. Yang, S. W. Xu, J. B. Ma, Q. Liu, Z. Bai, H. J. Ong, B. F. Lv, S. Guo, X. H. Wang, R. H. Li, M. K. Raju, Z. G. Hu, and H. S. Xu (RIBLL Collaboration), *Phys. Rev. C* **105**, 054616 (2022).
- [47] E. Bauge, J. P. Delaroche, and M. Girod, *Phys. Rev. C* **63**, 024607 (2001).
- [48] D. Y. Pang, Y. L. Ye, and F. R. Xu, *Phys. Rev. C* **83**, 064619 (2011).
- [49] B. A. Brown, *Phys. Rev. C* **58**, 220 (1998).
- [50] C. De Jager, H. De Vries, and C. De Vries, *At. Data Nucl. Data Tables* **14**, 479 (1974).
- [51] J. A. Tostevin and A. Gade, *Phys. Rev. C* **103**, 054610 (2021).